

Near surface mounted CFRP strips for the flexural strengthening of RC columns: Experimental and numerical research

Joaquim A.O. Barros^{a,*}, Rajendra K. Varma^a, José M. Sena-Cruz^a, Alvaro F.M. Azevedo^b

^a Department of Civil Engineering, University of Minho, Azurém, 4800-058 Guimarães, Portugal

^b Department of Civil Engineering, University of Porto, Rua Dr. Roberto Frias, 4200-465 Porto, Portugal

ARTICLE INFO

Article history:

Received 21 March 2007

Received in revised form

24 January 2008

Accepted 19 May 2008

Available online 27 June 2008

Keywords:

Near surface mounted reinforcement

Reinforced concrete columns

Strengthening

Carbon fiber reinforced polymer strips

Bending failure

Epoxy adhesive

ABSTRACT

In this work, a strengthening technique based on near surface mounted (NSM) carbon fibre laminate strips bonded into slits opened on the concrete cover is used to improve the flexural capacity of columns subjected to bending and compression. This technique avoids the occurrence of the peeling phenomenon, is able to mobilize the full strengthening capacity of the strips, and provides higher protection against fire and acts of vandalism. We describe the adopted strengthening technique and report the experimental characterization of the materials involved in the strengthening process. The results obtained in two series of reinforced concrete columns, subjected to axial compression and lateral cyclic loading, show that a significant increase on the load carrying capacity can be achieved by using the NSM technique. Cyclic material constitutive laws were implemented in a finite element program and the tests with reinforced concrete columns strengthened with the NSM technique were numerically simulated under cyclic loading. These numerical simulations reproduce the experimental load–displacement diagrams satisfactorily.

© 2008 Elsevier Ltd. All rights reserved.

1. Introduction

Until the last quarter of the twentieth century seismic loading was not generally taken into account in the design of reinforced concrete buildings or, when considered, the resulting reinforcement detailing might not be satisfactory by the standards of the current structural codes. For this reason, significant damage can occur in old buildings, even with the occurrence of moderate seismic loads. In most cases, columns represent the most vulnerable elements since their failure leads to the collapse of the structure.

Since the beginning of the nineties conventional materials used to strengthen reinforced concrete (RC) columns are being replaced with carbon and glass fibre reinforced polymers (CFRP or GFRP). The advantages of these composite materials are the strength/weight and stiffness/weight high ratios, as well as the high resistance to environmental actions, lightness, durability and ease of application [1–4].

In this work a strengthening technique, based on the installation of strips of carbon fibre reinforced polymer (CFRP) laminates into slits opened on the concrete cover of the elements

to strengthen, is used to increase the flexural resistance of RC columns failing in bending. These strips have a cross section of $9.6 \times 1.5 \text{ mm}^2$ and are bonded to concrete by means of an epoxy adhesive. This technique is termed near surface mounted (NSM) and its effectiveness in the flexural and shear strengthening of RC beams has been already assessed [5–10].

In recent years a significant amount of research has been undertaken with the aim of accurately modelling the cyclic behaviour of RC columns. An extensive review of available constitutive models and appropriate FEM-based numerical strategies is published elsewhere [11]. The most common approaches regarding the modelling of RC columns with finite elements involve a discretization with 3D solid elements or with Timoshenko beam elements. When 3D solid elements are used, some elements represent concrete and others simulate the reinforcement. For the case of Timoshenko beam elements each cross section is discretized into fibers, corresponding some to the concrete and the remaining to the reinforcement [12]. Models based on 3D solid elements are more suitable to reproduce the behaviour of RC columns subjected to any type of loading such as significant shear forces or torsion. Timoshenko beam based models are less demanding in terms of computational resources but are more appropriate to the simulation of columns mainly subjected to axial and flexural forces.

In the present work, the effectiveness of the NSM technique in the flexural strengthening of RC columns was appraised by means of two series of tests, with different steel reinforcement ratios, subjected to cyclic loading and constant axial compressive

* Corresponding author. Tel.: +351 2535 10210; fax: +351 2535 10217.

E-mail addresses: barros@civil.uminho.pt (J.A.O. Barros), rajendra@civil.uminho.pt (R.K. Varma), jsena@civil.uminho.pt (J.M. Sena-Cruz), alvaro@fe.up.pt (A.F.M. Azevedo).

Notations

The following symbols were used in the paper. Subscript *s* and *c* denote steel and concrete respectively.

C/T	Compression /Tension
$E_{c/s}$	Initial Young modulus of concrete/steel
$E_{cnew}^{+/-}$	Tangent modulus at the new stress point
$E_{so}^{+/-}$	Initial Young's modulus at reversal C/T branch
E_{cpl}	Tangent modulus when the stress is released
$E_{cre}^{-/+}$	Tangent modulus at the returning point ($\epsilon_{cre}^{-/+}, f_{cre}^{-/+}$)
E_{sc}	Tangent modulus of steel
$E_{sh}^{-/+}$	Tangent modulus at strain hardening ($\epsilon_{sh}^{-/+}$)
E_{st}	Tangent modulus of steel
$E_t^{-/+}$	Tangent modulus for concrete on C/T envelope
$f_{c/s}$	Concrete/steel stress
f_{ct}	Peak concrete tension strength
f'_c	Peak confined concrete strength
$f_c^{-/+}$	Concrete stress on the C/T envelope
$f_{cnew}^{-/+}$	New stress at the unloading strain for C/T
$f_{cre}^{-/+}$	Stress at the returning strain ($\epsilon_{cre}^{-/+}$)
$f_{csu}^{-/+}$	Ultimate (maximum) stress during C/T in steel
$f_{cun}^{-/+}$	Unloading stress from C/T concrete envelope curve
$f_{sy}^{-/+}$	Yield stress during C/T in steel
$n_c^{-/+}$	<i>n</i> value for the C/T envelope curve
$R_{so}^{+/-}$	Menegotto–Pinto Eq. parameter
χ_{csp}	Non-dimensional spalling strain
$\chi_c^{-/+}$	Non-dimensional strain on the C/T envelope
$\chi_{cr}^{-/+}$	Non-dimensional critical strain on C/T envelope curve.
ϵ_c	Concrete strain
ϵ'_c	Concrete strain at peak confined stress
$\epsilon_{so}^{-/+}$	Point of origin of the C/T envelope curve
ϵ_{cpl}	Plastic strain
$\epsilon_{cre}^{-/+}$	Strain at the returning point to the C/T envelope curve
$\epsilon_{sh}^{-/+}$	Hardening strain during C/T in steel
$\epsilon_{su}^{-/+}$	Strain at ultimate stress ($f_{su}^{-/+}$)
ϵ_t	Strain at peak tension stress
$\epsilon_{cun}^{-/+}$	Unloading strain from C/T concrete envelope curve

load. These tests were numerically simulated with the materially nonlinear algorithms of the FEMIX computer code [13]. In the context of this work, additional cyclic constitutive material models were developed and implemented in the code. The RC columns are discretized with 3D Timoshenko beam elements and each cross section is treated as a set of quadrilateral sub domains (fibrous model, [12]).

In the following sections the experimental and numerical research are described and the main results are presented and discussed.

2. Experimental program

The experimental program carried out in the context of the current work is composed of eight specimens and twelve tests as shown in Table 1. Two series of columns reinforced with longitudinal steel bars of 10 and 12 mm diameter, ϕ_l , were used. The following denominations are adopted: NON series for non-strengthened columns; PRE series for concrete columns strengthened with CFRP strips; POS series for columns of the NON

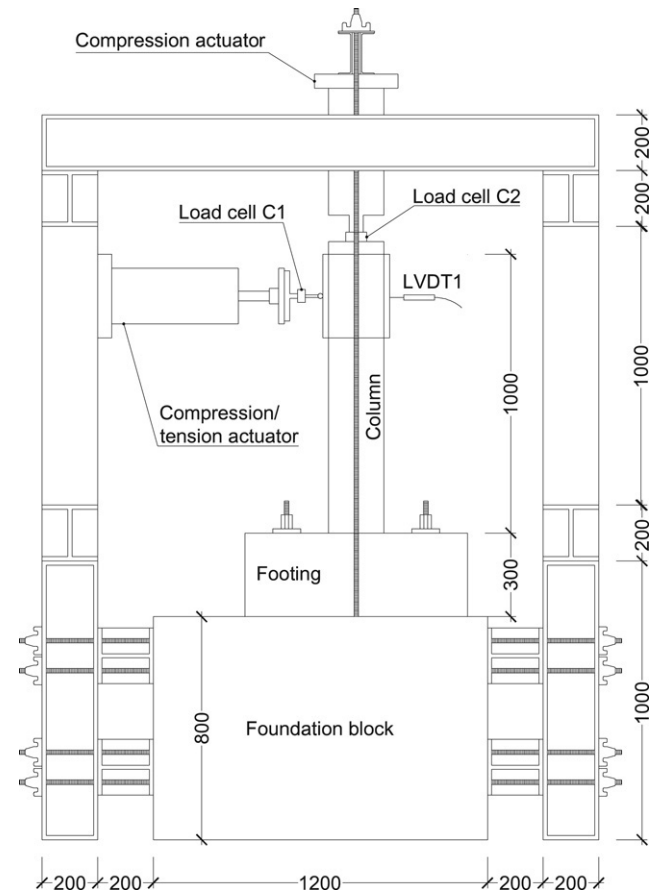


Fig. 1. Test set-up (dimensions in mm).

series which were strengthened and then retested. The generic denomination of a series is *Cnm_s*, where *n* represents the diameter of the longitudinal bars, in mm, (10 or 12), *m* is equal to *a* or *b* (*a* and *b* are two tests in similar conditions for statistical purposes), and *s* is equal to NON, PRE or POS.

3. Test setup and testing procedures

The test setup is shown in Fig. 1. Each specimen is composed of a column monolithically connected to a footing, which is fixed to a foundation block by four steel bars. The cyclic horizontal load was applied by means of an actuator having a load capacity of 100 kN. The force was measured using a tension/compression load cell that can reach a maximum load of 250 kN with 0.05% accuracy. This load cell was attached to the piston of the actuator (cell C1 in Fig. 1). To avoid eccentric forces on the actuator, a 3D hinge was placed between the column and the load cell that measures the horizontal force. A vertical load of approximately 150 kN was applied to the column, which corresponds to an axial load ratio of 0.22. The vertical load was kept practically constant during the test by means of a 250 kN actuator. This actuator was supported by two bolted steel bars, which were fixed to the foundation block. The axial vertical force was measured with a 500 kN load cell with 0.5% accuracy (cell C2 in Fig. 1). Linear variable displacement transducers (LVDT) were used to record the horizontal displacements of the column, as well as an eventual vertical movement of the footing (see Fig. 2). The measuring stroke for each LVDT is indicated in parentheses (± 12.5 or ± 25 mm). The location of the strain-gauges (SG) which were glued to the CFRP strips is also indicated in Fig. 2.

The tests were carried out with closed-loop servo-controlled equipment. A displacement history was imposed to LVDT1, with

Table 1
Denominations for the specimens

Longitudinal reinforcement (1)	Series		
	NON ^a (2)	PRE ^b (3)	POS ^c (4)
4 ϕ 10	C10a_NON C10b_NON	C10a_PRE C10b_PRE	C10a_POS C10b_POS
4 ϕ 12	C12a_NON C12b_NON	C12a_PRE C12b_PRE	C12a_POS C12b_POS

^a Non-strengthened.

^b Strengthened before testing.

^c Columns of NON series after have been tested and strengthened.

Table 2
Maximum forces obtained in the columns of PRE series (strengthened before testing)

	Series PRE			
	C10a_PRE	C10b_PRE	C12a_PRE	C12b_PRE
Age ^a (days)	111	113	110	115
Average compressive strength ^a (MPa)	17.49	14.99	23.55	17.93
Tensile (kN)	37.14	40.63	44.13	39.81
Compressive (kN)	−38.54	−37.96	−43.66	−36.64

^a Values at the age of the columns at testing.

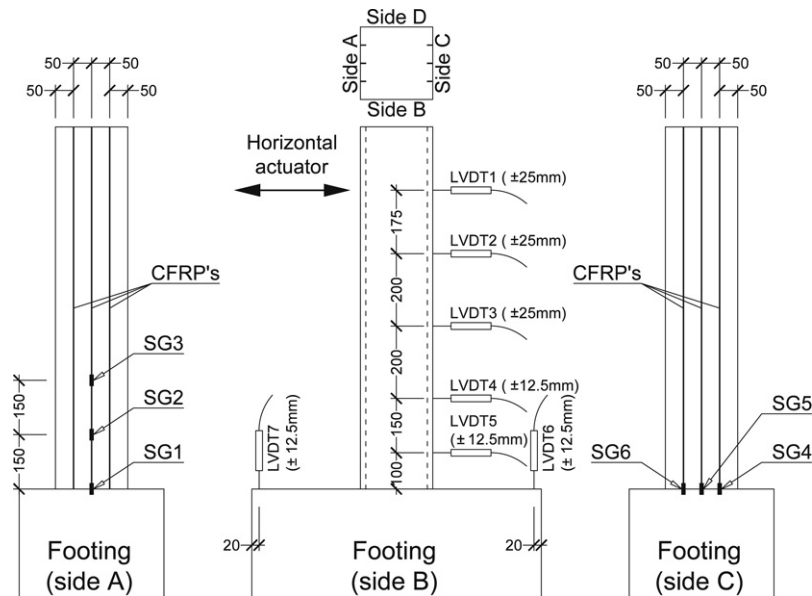


Fig. 2. Location of the displacement transducers (LVDT) and strain gauges (SG) (dimensions in mm).

a full range of 50 mm and 0.05% accuracy, located at the level of the horizontal actuator, see Fig. 1 and Fig. 2. From the analytical and numerical simulations it was verified that the steel yield initiation occurred for a lateral deflection of about 5 mm at the level of the horizontal actuator. Therefore, an increment of 2.5 mm was selected in the present experimental program. This increment was the same for all the specimens, in order to allow for the comparison of stiffness and strength degradation for the same lateral deflections. The displacement history included eight full loading-unloading cycles: ± 2.5 mm, ± 5.0 mm, ± 7.5 mm, ± 10.0 mm, ± 12.5 mm, ± 15.0 mm, ± 17.5 mm and ± 20.0 mm, with a displacement rate of 150 $\mu\text{m/s}$.

4. Material characterization

4.1. Concrete

A low strength concrete was used for all tests, in order to reproduce the type of concrete used in the sixties and seventies.

The concrete was composed of 250 kg/m^3 of normal Portland cement, 1196.5 kg/m^3 of gravel 5–15 mm, 797.5 kg/m^3 of sand 0–5 mm, and 151.5 l/m^3 of water.

The uniaxial compressive behaviour of the concrete of each column series was assessed by performing compression tests with two cylinders of 150 mm diameter and 300 mm height. These tests were performed at 28 days and at the time the columns were tested. For each series of columns, two beams with dimensions of 850 \times 100 \times 100 mm^3 were also cast for assessing the tensile strength in bending and the fracture energy of the concrete [14]. The results obtained in the compression tests indicated an average compressive strength, at 28 days, of 16.7 MPa, with a standard deviation of 3.31 MPa. An average tensile strength of 2.62 MPa, with a standard deviation of 0.48 MPa, and an average fracture energy of 0.08 N mm/mm^2 were registered from the three-point notched beam bending tests, at 28 days. Tables 2 and 3 include the values of the concrete compressive strength at the age of the column tests.

Table 3

Maximum forces obtained on the columns of series NON (non-strengthened) and POS (strengthened after preliminary testing)

Column		C10a_	C10b_	C12a_	C12b_
Diameter of longitudinal bars (mm)		10	10	12	12
Average compressive strength ^a (MPa)		15.21	13.21	17.23	19.95
Tensile	NON (kN)	16.67 (86) ^b	21.78 (85) ^b	26.35 (85) ^b	29.31 (85) ^b
	POS (kN)	37.96 (146) ^b	41.38 (130) ^b	34.11 (150) ^b	45.54 (154) ^b
	Increase (%)	127.7	89.99	29.45	55.37
Compressive	NON (kN)	−19.76 (86) ^b	−24.07 (85) ^b	−30.52 (85) ^b	−32.27 (85) ^b
	POS (kN)	−34.11 (146) ^b	−43.1 (130) ^b	−37.03 (150) ^b	−41.58 (154) ^b
	Increase (%)	72.62	79.06	21.33	28.85

^a Values at the age of the columns at testing of the series NON.^b Values inside round parentheses represent the age of the columns at testing, in days.**Fig. 3.** Adopted flexural strengthening technique for RC columns (dimensions in mm).

4.2. Steel reinforcement

In the RC structures built in the sixties and seventies smooth surface steel bars were commonly used. For this reason, this type of bars was also used in the reinforcement of the tested columns. To assess the behaviour of the steel bars, uniaxial tensile tests were carried out in a servo-controlled testing machine, according to the recommendations of the European standard EN 10 002 [15]. The yield stress (f_{sy}), the ultimate stress (f_{su}), and the elasticity modulus (E_s) of $\phi 6$ bars are (as an average of the tests with three specimens): $f_{sy} = 352.4$ MPa, $f_{su} = 352.8$ MPa, and $E_s = 203\,700$ MPa. The reinforcement details for $\phi 10$ and $\phi 12$ bars are presented later (see Table 6).

4.3. Epoxy mortar

An epoxy mortar was used to fix the CFRP laminates to the column footing (see Fig. 3). The epoxy mortar was composed of one part of epoxy and three parts of fine sand previously washed and dried (parts measured in weight). The uniaxial compressive strength and the flexural tensile strength of the epoxy mortar were evaluated from tests in specimens with $160 \times 40 \times 40$ mm³, at 48 h and at 28 days, following the European standard [16]. At 48 hours, a compressive strength of 43.75 MPa, with a standard deviation of 2.14 MPa, and a flexural tensile strength of 33.93 MPa with a standard deviation of 0.57 MPa, were obtained. At 28 days, a compressive strength of 51.71 MPa, with a standard deviation of 0.47 MPa, and a flexural tensile strength of 35.40 MPa, with a standard deviation of 1.70 MPa, were obtained.

In order to evaluate the adhesive properties of the epoxy mortar relatively to a concrete surface, the following procedure was undertaken: reutilization of the remains of previous bending tests with $850 \times 100 \times 100$ mm³ beams, which were used to evaluate the properties of the concrete used in the columns; utilization of the epoxy mortar to glue both pieces together; test of the resulting specimen under flexure load. In these tests it could be observed that the fracture neither propagated across the epoxy mortar, nor across its interface with the concrete (see Fig. 4). Therefore, these tests indicated that the properties of the bonding between the developed epoxy mortar and concrete are very good.

4.4. CFRP laminate strips

The CFRP strips, which were provided in rolls, had a thickness of 1.45 ± 0.005 mm and a width of 9.59 ± 0.09 mm (average values of 15 measures). To evaluate the tensile strength and the elasticity

Fig. 4. Notched beam bending tests for the characterization of the concrete-epoxy mortar bond performance: (a) test setup; (b) crack propagation.

